

Highly Mobile Oxygen Holes in Magnesium Oxide

Minoru M. Freund

Laboratorium für Festkörperphysik, Eidgenössische Technische Hochschule Hönggerberg, CH-8093 Zürich, Switzerland

Friedemann Freund and François Batllo^(a)

SETI Institute, NASA Ames Research Center, MS 239-4, Moffett Field, California 94035

(Received 21 August 1989)

High-purity MgO exhibits an unexpected giant anomaly of the apparent static dielectric constant and a positive surface charge of the order of $5 \times 10^{21} \text{ cm}^{-3}$ in the top 15 nm. We postulate that the MgO matrix contains traces of peroxy defects, O_2^{2-} , associated with Mg^{2+} vacancies. Above $\approx 400^\circ\text{C}$ the O_2^{2-} dissociates to vacancy bound O^- and highly mobile O^- states, which diffuse to the surface, giving rise to a high surface conductivity.

PACS numbers: 73.25.+i, 61.70.At, 77.20.+y

Even though high-purity MgO is a classical wide-band-gap insulator, it paradoxically exhibits an unusually high electrical conductivity at temperatures between 400 and 800°C .¹ We explain this by the existence of small concentrations (10–100 at. ppm) of highly mobile oxygen holes (O^- states in the O^{2-} sublattice), generated by the thermal dissociation of peroxy-type defects (O_2^{2-}). As observed for the first time, the products of this dissociation induce a very significant increase in the apparent static dielectric constant and a positive surface charge. We have measured both quantities with a new technique called charge distribution analysis (CDA).²

The O_2^{2-} are incorporated into the crystal during crystal growth by the dissolution of traces of H_2O in MgO.³ The most abundant defect expected from this dissolution is the fully OH^- -compensated cation vacancy $[\text{OH} \cdot V''_{\text{Mg}}\text{HO} \cdot]^\times$,⁴ where two protons substitute for an Mg^{2+} . The OH^- pair appears to be unstable in the vicinity of the cation vacancy: It undergoes an internal redox-type charge-transfer conversion,⁵ changing into an H_2 molecule plus a peroxy anion (O_2^{2-}): $[\text{OH} \cdot V''_{\text{Mg}}\text{HO} \cdot]^\times = [(\text{H}_2)''_{\text{Mg}}(\text{O}_2) \cdot]^\times$. Both defects are infrared active, the latter because the H_2 is weakly coupled to the π^* orbitals of the O_2^{2-} . Since H_2 molecules are diffusively mobile, they are easily removed, leaving behind bare cation vacancies compensated by tightly coupled (O-O distance $\approx 1.5 \text{ \AA}$) positive hole pairs $[V''_{\text{Mg}}(\text{O}_2) \cdot]^\times$. An O_2^{2-} represents two positive holes, localized on two adjacent O^{2-} sites,⁶ spin paired and thus diamagnetic. With the loss of the H_2 from the MgO matrix, spectroscopic evidence for the former presence of dissolved H_2O is lost.

The peroxy defect is susceptible to thermally activated dissociation. This occurs above $T_{\text{diss}} \approx 400^\circ\text{C}$ in the MgO lattice,⁶ $[V''_{\text{Mg}}(\text{O}_2) \cdot]^\times = [V''_{\text{Mg}}\text{O} \cdot] + \text{O} \cdot$, generating two positive hole-type defects: a V center, e.g., an O^- state which remains bound to the cation vacancy though it delocalizes over all six neighboring oxygens,⁷ and an unbound O^- state which represents a hole in the O-2p-dominated valence band.⁶ The unbound O^-

diffuses to the surface leading to a positive surface charge.⁶ Since Mg^{2+} diffusion in MgO is negligible at the temperatures of interest here,⁸ a positive surface charge can only be generated by positive holes. At the same time, in the absence of ionizing radiation,⁷ O^- states can only be generated by the dissociation of peroxy defects.

Using CDA we have studied the generation of mobile charge carriers in dielectrics. When a dielectric is placed in an external electric field of field strength \mathbf{E}_{ext} it becomes polarized and its polarization \mathbf{P} is given by

$$\mathbf{P} = \frac{\epsilon_0(\epsilon - 1)}{4\pi} \mathbf{E}_{\text{ext}}, \quad (1)$$

where ϵ_0 the permittivity of vacuum and ϵ the dielectric constant. The static dielectric constant is normally obtained by extrapolating to 0 Hz the values measured at moderate frequencies of 10^3 – 10^6 Hz. At 0 Hz, however, physical effects with long time constants of the order of hours can be probed. \mathbf{P} contains at least four contributions, $\mathbf{P} = \mathbf{P}_0 + \mathbf{P}_1 + \mathbf{P}_2 + \mathbf{P}_3$, which denote, respectively, (i) those from the ideal dielectric arising from the deformation of the electron clouds and the displacements of the nuclei, (ii) those from local dipoles which may rotate but not diffuse, (iii) those from mobile charges which can diffuse over macroscopic distances, and (iv) those from surface states alone, for an isotropic dielectric.

By placing a dielectric in a static inhomogeneous electric field (with a field gradient along the z direction) we generate a force \mathbf{F}_z causing an attraction towards the region of higher electric field density. The force $\mathbf{F}^\pm \equiv \mathbf{F}_z(\pm \mathbf{E}_{\text{ext}})$ can be calculated by using the Maxwell equations:

$$\mathbf{F}^\pm = - \int_V (\mathbf{P} \cdot \nabla) \mathbf{E}_{\text{ext}} dV, \quad (2)$$

where the integral over the volume V includes the sample but not the sources of the field.

For isotropic dielectrics with only bulk contributions (\mathbf{P}_0 , \mathbf{P}_1 , and \mathbf{P}_2) one finds using Eq. (1) $\mathbf{F}^\pm \propto \epsilon - 1$.

Since \mathbf{E}_{ext} is proportional to the potential difference U between the electrodes, $\mathbf{F}^{\pm} \propto U^2$. By contrast surface contributions from \mathbf{P}_3 cause the dielectric to be either attracted to or repelled from the region of higher electric field density, depending upon the sign of the surface charge and polarity of the field. It is possible to separate the contributions to the forces \mathbf{F}^{\pm} from the bulk and from the surface by forming, respectively, the linear combinations \mathbf{F}_{Σ} and \mathbf{F}_{Δ} , where

$$\mathbf{F}_{\Sigma} \equiv \frac{1}{2} (\mathbf{F}^+ + \mathbf{F}^-) = -\frac{\epsilon_0(\epsilon - 1)}{4\pi} \int_V \nabla E_{\text{ext}}^2 dV, \quad (3)$$

$$\mathbf{F}_{\Delta} \equiv \frac{1}{2} (\mathbf{F}^+ - \mathbf{F}^-) = -\int_V (\mathbf{P}_3 \cdot \nabla) \mathbf{E}_{\text{ext}} dV. \quad (4)$$

A Perkin-Elmer TGS-1 was used for the present experiments, equipped with a Cahn microbalance as a force-measuring device and a cup-shaped furnace on alumina ceramic, 6 mm inner diameter and 10 mm depth, with induction-free bifilar Pt windings, acting as a cylindrical electrode. We report here on arc-fusion-grown MgO single crystals of nominal purity grades 99.9% and 99.99% containing traces (10–100 at. ppm) of dissolved H_2O and possibly⁵ CO and CO_2 . The MgO crystals were cylindrical plates 4 mm in diameter and 1–2 mm thick. The samples were suspended from a fused silica fiber, well insulated from ground, and positioned so that their upper (100) surface was level with the furnace rim. A Ni bias electrode (3×5 mm) was introduced sideways above the sample, parallel to the sample surface at a distance of 0.5–1 mm. The temperature was calibrated by means of the Curie points of ferromagnetic alloys. All experiments were carried out under Ar flowing at 40 ml/min. The MgO crystals were heated at 40°C/min to constant temperature levels and kept there for 3–5 min to thermally equilibrate. Cooling between temperature steps was done at 10 or 20°C/min. With different bias voltages the forces \mathbf{F}^{\pm} were recorded as apparent weight changes of the sample. From this we calculated \mathbf{F}_{Σ} and \mathbf{F}_{Δ} .

Figure 1(a) shows the variation of \mathbf{F}_{Σ} up to 900°C. The dotted line corresponds to the force measured within 3 min after application of ± 75 V. For long times \mathbf{F}_{Σ} reaches asymptotically the saturation value given by the solid line. The observed increase in the polarization appears as an increase of the apparent dielectric constant, $\mathbf{F}_{\Sigma} \propto \epsilon - 1$. Literature values⁹ for the static ϵ of MgO vary between 7 and 9.6. The increase of \mathbf{F}_{Σ} is about eighteenfold, corresponding to an increase of ϵ to about 140–150. This increase in the apparent ϵ is due to free charge carriers, implicating a macroscopic conduction mechanism, unlike the microscopic polarization found in other dielectrics.

In Fig. 1(b) we plot the variation of $-\mathbf{F}_{\Delta}$ up to 900°C. The MgO surface is negatively charged below $T_{\text{diss}} \approx 400^\circ\text{C}$. The magnitude of this charge sensibly depends upon the cooling rate from previous experiments

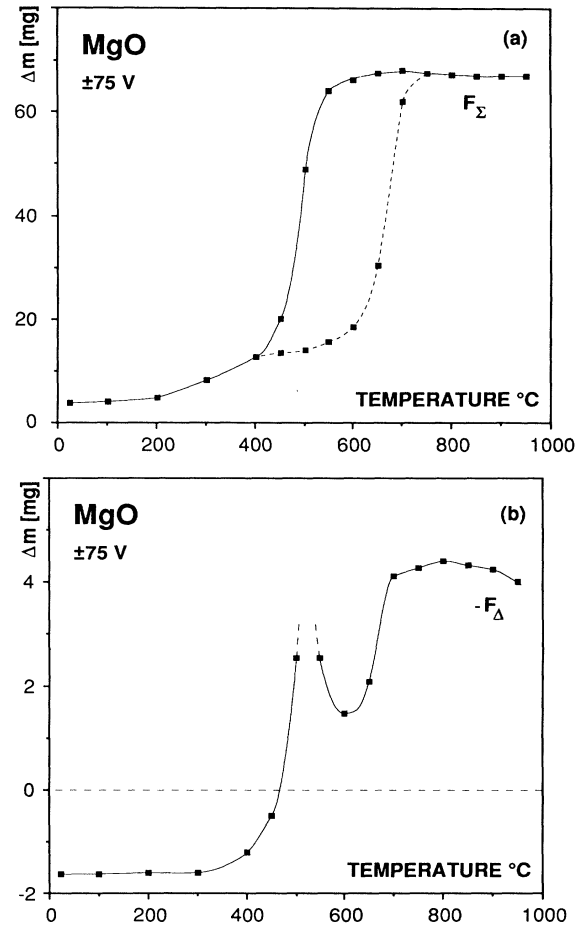


FIG. 1. (a) Apparent dielectric constant and (b) surface charge as a function of temperature, expressed as the forces \mathbf{F}_{Σ} and $-\mathbf{F}_{\Delta}$. (Note that for this geometry a negative value of \mathbf{F}_{Δ} corresponds to a positive value of the surface charge.) The dashed line corresponds to values for about 3 min after reaching the indicated temperature, and the solid line to saturation values for very long time.

and many represent the intrinsic charge state of the MgO surface.¹⁰ Above T_{diss} the surface charge turns suddenly positive. Between T_{diss} and 600°C \mathbf{F}_{Δ} shows a similar time dependence as \mathbf{F}_{Σ} . Above 600°C the positive surface charge stabilizes. Both \mathbf{F}_{Σ} and \mathbf{F}_{Δ} are readily reversible upon slow to moderately fast cooling, indicating that the recombination $[\text{V}''_{\text{MgO}}] + \text{O}_\bullet \rightleftharpoons [\text{V}''_{\text{Mg}}(\text{O}_2)]^\times$ is reversible. The measured forces show a strong time dependence between 400 and 700°C. Above 700°C, however, these processes are too fast to be observed. This is consistent with a diffusion model for the oxygen holes, as we shall report in a forthcoming paper.

Using the measured values for \mathbf{F}_{Δ} we can calculate approximately the surface charge density. According to King and Freund⁶ and using corrections estimated by Yan, Cannon, and Bowen¹¹ the surface dipole layer of

unbound O^- states in MgO is ≈ 30 nm wide. Assuming a cylindrical geometry we place two such dipole layers at both surfaces perpendicular to the z direction of a crystal and neglect all charges on the sides of the cylinder. Using the fact that E_{ext} only depends on the geometry, F_{Δ} is given by

$$F_{\Delta} = 8\pi^2 \epsilon_0 U (Ne) \frac{D^2}{a^2} \sum_{n=1}^{\infty} \beta_n \left[\int_0^b \rho J_0(k_{0n}\rho) d\rho \right] \{ \cosh(k_{0n}g) - \cosh[k_{0n}(g+c)] \}, \quad (5)$$

where

$$\beta_n = k_{0n} \frac{\text{cosech}(k_{0n}L)}{J_1(k_{0n}a)} \left[\int_0^d \rho J_0(k_{0n}\rho) d\rho \right],$$

D the dipole layer thickness, $2a$ the diameter of the cylindrical counter electrode, L the length of the cylindrical counter electrode, $2b$ the diameter of the sample, c the sample thickness, $2d$ the diameter of the bias electrode, g the distance of sample-bias electrode, N the number of electric charge carriers per unit area, e the electric charge of the carriers, and ϵ_0 the permittivity of the vacuum. J_n are the Bessel functions of n th order, where $k_{0n} = x_{0n}/a$, with x_{0n} being the solutions of the zero-order Bessel function $J_0(x_{0n}) = 0$. Inserting the experimental values and solving for N in Eq. (5) we find that 5%–10% of the O^{2-} in the first 15 nm of the surface layer must have converted to O^- . This corresponds to a charge-carrier density within this surface layer of $\approx 5 \times 10^{21} \text{ cm}^{-3}$. Taking into account both the errors made by the approximations and the experimental errors for the parameters, we estimate that the calculated surface charge density should be correct to within about 1 order of magnitude.

In Fig. 2 we plot F_{Σ} and F_{Δ} vs U as measured at 650°C along with the raw data F^+ and F^- . Since $P_0 + P_1 + P_2 \propto U$, $F_{\Sigma} \propto U^2$. By contrast F_{Δ} , which describes the surface term, first decreases linearly as a

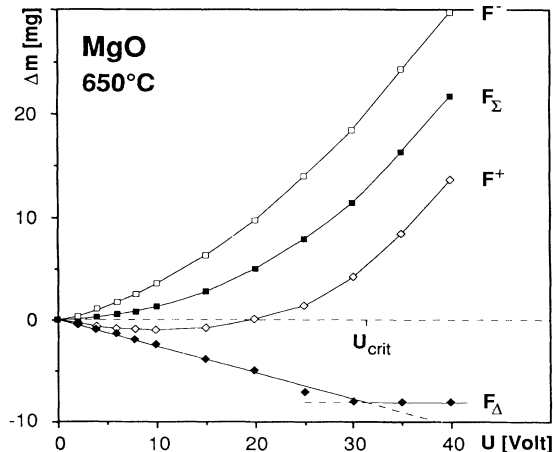


FIG. 2. Polarity-invariant response F_{Σ} and response due to a positive surface charge F_{Δ} at constant temperature as a function of the bias voltage. (Also shown are experimental raw data curves F^+ and F^- under positive and negative bias, respectively.)

function of U , $F_{\Delta}/U \propto Ne$, and then becomes independent of U above U_{crit} . Thus the surface charge responsible for P_3 is constant up to U_{crit} . This is consistent with a valence band which bends downwards close to the surface and traps O^- . The positive bias voltage raises the energy of the surface states until they merge with the bulk valence band at U_{crit} . Above U_{crit} , when $P_3 \propto 1/U$, the surface O^- layer acts like a spring-loaded charge which recedes into the bulk. U_{crit} reaches its highest value around $750\text{--}800^\circ\text{C}$ but decreases above 800°C , probably as a result of the onset of ionic conduction.

The presence of mobile holes in wide-band-gap insulators like MgO might affect many of our fundamental views on this class of substances. We shall discuss just a few examples. First, we note that the high density of mobile surface carriers is likely to cause a high surface conductivity. Indeed, the conductivity of nominally highest-purity MgO crystals increases drastically by several orders of magnitude between 400 and 650°C .¹ Strong conductivity spikes were observed, indicating electric short circuiting across the surface. Second, we note that O^- states are chemically reactive. In the bulk they can cause oxidation of transition-metal cations.¹² At the surface they may also disproportionate and release oxygen: $O_{O^\cdot} + O_{O^\cdot} = V_{O^\cdot} + O_{O^\cdot}^x + \frac{1}{2} O_2 \uparrow$, where V_{O^\cdot} and $O_{O^\cdot}^x$ represent, respectively, an O^{2-} vacancy and an O^{2-} on a regular O^{2-} site. Furthermore, surface O^- can oxidize gases such as H_2 and CO to H_2O and CO_2 , annihilating mobile charge carriers and reducing the surface conductivity. Preliminary experiments using Ar- O_2 , Ar- H_2 , and Ar- CO mixtures indicate that CDA is a useful technique to study such reactions. Third, these redox processes might serve to understand the exchange of oxygen in high- T_c superconductors.¹³ Moreover, the physics of peroxy defects in MgO might serve as a model for oxygen-related defects and improve the understanding of the conduction mechanisms in the high- T_c superconductors.¹⁴

In conclusion, we found from CDA experiments a dramatic increase in the apparent static dielectric constant and a positive surface charge of MgO above $\approx 400^\circ\text{C}$. We interpret this by a thermally activated dissociation mechanism of peroxy defects in the bulk above $T_{\text{diss}} \approx 400^\circ\text{C}$. The dissociation leads to a new electrical conduction mechanism by highly mobile and reactive charge carriers in otherwise wide-band-gap insulators.

This work was supported in part by the NASA/SETI Cooperative Agreement NCC 2-446. We acknowledge

the technical assistance of R. C. LeRoy. We thank T. Wydeven and S. Chang for stimulating discussions.

^(a)Permanent address: Chimie des Solides, Université de Bourgogne, F-21004 Dijon, France.

¹H. Kathrein and F. Freund, *J. Phys. Chem. Solids* **44**, 177 (1983).

²F. Freund, M. M. Freund, and F. Batllo, in "Spectroscopic Characterization of Mineral and Mineral Surfaces," edited by L. Coyne, S. McKeever, and D. F. Blake (American Chemical Society, Washington, DC, to be published).

³K. L. Kliewer and J. S. Koehler, *Phys. Rev.* **140**, A1226 (1965).

⁴Following Kröger [F. A. Kröger, *The Chemistry of Imperfect Crystals* (North-Holland, Amsterdam, 1964)] superscript prime, dot, and cross stand for a negative, positive, and neutral charge, respectively, referenced to the ideal structure. Subscripts specify the lattice sites. Square brackets include the

essential elements of the point defect.

⁵F. Freund and H. Wengeler, *J. Phys. Chem. Solids* **43**, 129 (1982).

⁶B. V. King and F. Freund, *Phys. Rev. B* **29**, 5814 (1984).

⁷J. E. Wertz and B. Henderson, *Defects in the Alkaline Earth Oxides* (Taylor and Francis, London, 1977).

⁸J. H. Harding and A. H. Harker, *Philos. Mag. B* **51**, 119 (1985).

⁹J. S. Thorp, N. E. Rad, D. Evans, and C. D. H. Williams, *J. Mater. Sci.* **21**, 3091 (1986).

¹⁰W. D. Kingery, *J. Am. Ceram. Soc.* **57**, 1 (1974), and references therein.

¹¹M. F. Yan, R. M. Cannon, and K. H. Bowen, *J. Appl. Phys.* **54**, 764 (1983).

¹²H. Kathrein, J. Nagy, and F. Freund, *J. Phys. Chem. Solids* **45**, 1155 (1984).

¹³See, for example, J. Karpinski *et al.*, *Nature (London)* **331**, 242 (1988).

¹⁴J. E. Hirsch, S. Tang, E. Loh, and D. J. Scalapino, *Phys. Rev. Lett.* **60**, 1668 (1988).